Differential angular distribution of prompt gamma rays from spontaneous fission of ^{252}Cf

K. Skarsvåg
Institutt for Atomenergi, Kjeller Research Establishment, 2007 Kjeller, Norway
(Received 23 October 1979)

The differential angular distribution of prompt γ rays from spontaneous fission of ^{252}Cf has been measured. The source was on a thick backing, and the measurements have been performed in forward and backward geometries. An NaI(Tl) crystal was used as a γ-ray detector, and the prompt neutrons from fission were rejected by time of flight. The total number of γ rays emitted within 12 ns after fission with energies greater than 0.114 MeV is 9.7 ± 0.4 per fission, and the total γ-ray energy released is (7.0 ± 0.3) MeV per fission. Results from earlier experiments that more γ rays are emitted from the light than from the heavy fragment group, are substantiated. The anisotropy $A = I(0°)/I(90°) - 1$ is small and even negative at low energies, reaches a maximum of about 25% at energies of about 0.50–0.65 MeV, and gets gradually smaller at higher energies. No significant difference in the anisotropy as measured with a nonmagnetic (Pt) and a magnetic (Ni) backing has been found. With the assumption that the angular momentum is aligned in a plane perpendicular to the direction of fission, the results can be consistently described within the statistical model in terms of pure dipole and quadrupole radiation with allowance for stretched $E2$ cascades from even-even fragments. It is concluded that the root mean square value of the primary angular momentum of the fragments is $J_{\mathrm{rms}} = (6.5 \pm 1.0)\hbar$, the average angular momentum is decreasing $1.0\hbar$ per γ ray emitted, and the value of the spin cutoff parameter during γ-ray deexcitation of the fragments is $\sigma = 2.4^{+0.8}_{-0.5}$. The dipole and the quadrupole components are about equally strong at high γ-ray energies, the dipole component predominates at low energies, and the quadrupole component at intermediate energies. Statistical dipole and quadrupole transitions (stretched for the last ones) account for 38% and 50% of the γ rays, respectively, and stretched $E2$ transitions in cascades from even-even fragments account for the remaining 12% of the γ rays. The quadrupole radiation can be assumed to be $E2$, and the dipole radiation $M1$ at low energies and $E1$ at high energies. While the components of the stretched $E2$ cascades with energies smaller than 0.6 MeV can be accounted for by the transitions in the ground-state rotational bands of even-even fragments, it is indicated that a large part of the components in the energy range 0.6–0.9 MeV can be associated with vibrational transitions in even-even fragments.

[RADIOACTIVITY, FISSION ^{252}Cf (sf); measured $\sigma(E_\gamma, \theta)$ of γ from fragments, $N_{\gamma,\mathrm{tot}}$, $E_{\gamma,\mathrm{tot}}$, $N_{\gamma H}$, $N_{\gamma L}$; deduced $\bar{J}$, yield of various multipolarities.]

I. INTRODUCTION

The angular distribution of the γ rays from fission with respect to the fission direction can give information about quantities such as the multipolarity of the radiation and the magnitude and alignment of the angular momentum of the fragments.[1]

The angular distribution of the integral spectrum has been extensively measured (see, e.g., works cited in Ref. 1), but only few differential measurements have been performed.[2,3] Angular distributions of specific[4] γ rays have also been measured in a limited number of cases amounting to about 5% of the whole spectrum. Only one systematic study of the influence of nonmagnetic (Pt) *contra* magnetic (Fe) backing materials has been made.[3]

A forward-backward anisotropy of γ rays from a source on a thick backing relative to the direction of the fragments in flight has been found from measurements with the source on the backing facing the γ-ray detector (forward geometry) and turning away from it (backward geometry).[5-7] This anisotropy is mainly due to the solid angle aberration and the Doppler shift in energy of the γ rays, and is thus dependent upon the average emission time[7,8] of the γ rays relative to the stopping time of the fragments.

In this paper we present the results of the measurements of the differential angular distribution of prompt γ rays from spontaneous fission of ^{252}Cf as obtained in forward and backward geometries and for a nonmagnetic (Pt) and a magnetic (Ni) backing.

II. METHOD

We define $W(\theta)$ and $W'(\vartheta)$ as the number of γ rays per γ ray per unit solid angle in the center of mass and in the laboratory system, respectively. We have

$$W'_{DF}(\vartheta) = T_{DF} W(\theta) , \tag{1}$$

where

$$T_{DF} = (1 - \beta_{DF}^2)/(1 - \beta_{DF}\cos\vartheta)^2 . \tag{2}$$

Here θ and ϑ are the angles between the propagation vector of the photon and the velocity of the fragment in the c.m. and lab systems, respectively, and β_{DF} is the time average of the velocity of the fragment in units of c. The first index $(D=V,B)$ refers to fragments going out of and into the backing, respectively, and the second one $(F=H,L)$ refers to the fragment group (heavy or light) from which the γ ray is emitted. We also have

$$\sin\theta_{DF}=T_{DF}\sin^2\vartheta_{DF}. \tag{3}$$

Let $c_H(c_L)$ be the number of γ rays per N_0 heavy (light) fragment counts, where N_0 here will be taken as 10^7. We then get for the angular distribution of γ rays gated by the heavy and the light fragments, respectively,

$$Z_H(\vartheta)=c_H S_{VH}W(\theta_{VH})+c_L S_{BL}W(\theta_{BL}), \tag{4a}$$

$$Z_L(\vartheta)=c_H S_{BH}W(\theta_{BH})+c_L S_{VL}W(\theta_{VL}), \tag{4b}$$

where the angle ϑ is taken relative to the velocity of the fragment which is counted, $Z_H(\vartheta)$ and $Z_L(\vartheta)$ are the numbers of γ rays per unit solid angle per N_0 fragment counts, and S_{DF} is a transformation and correction function.

For γ rays emitted from fragments which are counted, the function is to first order

$$S_{VF}=1+2c_{VF}g\beta_F\cos\vartheta +2[c_{VF}(c\tau/D)\beta_F+(1-c_{VF})(d/D)]\cos\vartheta. \tag{5}$$

The first linear term arises from the solid angle aberration [cf. Eqs. (1) and (2)] and the Doppler shift in energy of the γ rays. Here β_F is the average initial fragment velocity[9] ($\beta_H=0.03449$ and $\beta_L=0.04570$), c_{VF} is the fraction of the γ rays emitted from the fragments before being stopped in the detector, and the correction factor g is[7]

$$g=1+\tfrac{1}{2}(f_L-f_U), \tag{6}$$

where f_L and f_U are the ratios between the incremental relative change in counting rate and the incremental relative change in energy at the lower and upper limit of the γ-ray energy interval, respectively. The second linear term takes into account the change in solid angle of the γ-ray detector as seen from the fragments. Here τ is the average mean lifetime,[7,8] D is the distance between source and γ-ray detector, and d is the distance between source and fragment detector.

The corresponding function for γ rays emitted from fragments going into the backing is

$$S_{BF}=1-2gF_B\beta_F\cos\vartheta, \tag{7}$$

where F_B is the velocity attenuation factor in the backing.[7] Alternatively the two Eqs. (4a) and (4b) are added together

$$Z_F(\vartheta)=c_F[S_V W(\theta_V)+S_B W(\theta_B)], \tag{4c}$$

in which case the quantities θ_V, θ_B, S_V, and S_B are average values of the corresponding quantities in Eqs. (4a) and (4b).

The angular distribution in the c.m. system is expanded as usual in Legendre polynomials

$$W(\theta_{DF})=1+A_{2F}P_2(\cos\theta_{DF})+A_{4F}P_4(\cos\theta_{DF}). \tag{8}$$

The theoretical expressions (4a) and (4b) [or (4c)] are fitted to the measured angular distributions of the γ rays in the various energy intervals by the method of iterative least-squares analysis.

III. EXPERIMENTAL SETUP

The experimental arrangement is shown in Fig. 1. The γ-ray detector was an NaI(Tl) crystal, 12.7 cm in diameter and 10.2 cm thick, mounted on an XP 1040 photomultiplier, and the distance between the ^{252}Cf source and the face of the γ-ray detector was 90.3 cm. The vacuum chamber with the source and the fragment detector was mounted on a turntable, which could be turned 180° about a vertical axis through the source from the forward to the backward geometry and vice versa. The fission fragment detector and the γ-ray detector could both be seen at an angle of 45° relative to the normal of the backing of the source. The angle between the detectors as seen from the source, could be varied by pivoting the vaccum chamber about an axis through the center of the source normal to the backing. Two different ^{252}Cf sources were used in the experiment. One of them was on a magnetic (Ni) backing 22 mg/cm^2 thick and the

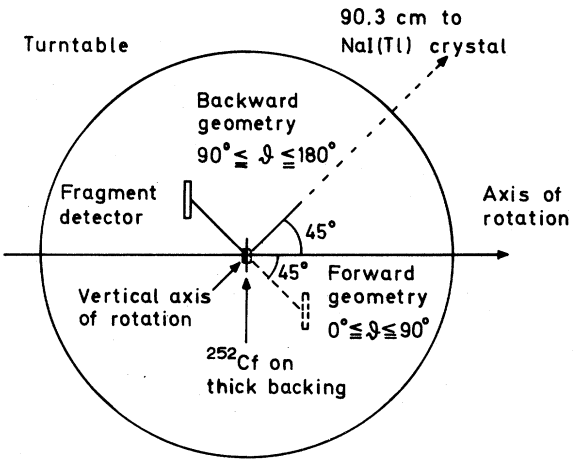

FIG. 1. Experimental arrangement.

other one on a nonmagnetic (Pt) backing 114 mg/cm^2 thick. The latter source had a protecting layer of NiCr of about 100 μg/cm^2 thickness. The strength of the former source was about 4×10^4 fissions/min and of the latter about 2×10^4 fissions/min. The fragment detector, which was an Ortec surface barrier detector 300 mm^2 in area, was mounted at a distance of 3.7 cm from the source. The detector was in thermal contact with a cold finger which was kept at a temperature of −18 °C by a Peltier module. The thickness of the backing in the backward geometry as traversed by the γ rays detected is independent of the angle in this geometry. The thickness of the fragment detector in the forward geometry as seen from fragments stopped in the detector will also be independent of the angle.

A time-to-amplitude converter assembly gave a time-of-flight spectrum with a time resolution full width at half maximum (FWHM) of about 5 ns for the integral spectrum above 0.10 MeV. Pulses from −12 to +12 ns were accepted in the measurements, and the γ-ray pulse-height distributions associated with the heavy and the light fragment group were stored in the two halves of a 400 channel analyzer in the energy range 0.10–2.54 MeV. Events with γ-ray energy greater than 2.54 MeV were counted, but not pulse-height analyzed. The bias defining the limit between the heavy and the light fragment group was stabilized to make the number of fragment counts in the two groups nearly equal at any time.

Measurements were done at five forward angles (30°, 45°, 60°, 75°, and 90°) and six backward angles (90°, 120°, 135°, 150°, 165°, and 180°). The total time used at each angle was between one and two weeks. The performance of the fragment detector degraded due to radiation damage and was replaced twice.

The efficiency, energy, and resolution of the NaI(Tl) detector were determined using standard sources in the 0.122–1.836 MeV range. The efficiency as a function of energy was extrapolated to higher energies by means of calculated values given in Ref. 10.

The fraction c_{RF} of the γ rays emitted from the fragments after being stopped in the detector ($c_{RF} = 1 - c_{VF}$) was estimated from previous measurements,[8] and confirmed in an auxiliary measurement with and without a shield between the two detectors. The fraction c_{RF} goes from 0.14 at 0.13 MeV to 0.04 at 0.38 MeV and is neglected for energies above 0.42 MeV.

IV. ANALYSIS

The measured γ-ray pulse-height distributions normalized to 10^7 heavy (or light) fragment counts were initially divided into 21 groups with the number of channels in each group about proportional to the energy resolution,[7] and the remaining counts were then stored in the 22nd group. The distributions formed by 22 groups for each fragment group at each angle were transformed by the inverse response matrix of the NaI(Tl) detector generated in a similar way as described by Pleasonton *et al.*[11] This data set gave the angular distribution in 22 energy intervals. The energy distribution within each group was assumed to be proportional to the corresponding distribution in the original data, and the correction factors g, defined by Eq. (6), could then be found. They were taken as the average over three forward angles (30°, 60°, and 90°) and three backward angles (90°, 120°, and 150°) and go from about zero at low energies to about 1.8 at higher energies in fair agreement with earlier results (see Fig. 5 in Ref. 7). The groups 16–18 and 19–21 were subsequently combined in order to improve the statistics within each group, which reduces the number of groups to 18 ($K = 1$–18).

The coefficients $A_k (k = 2.4)$ were corrected for the finite solid angle subtended by the detectors through the solid-angle correction factors Q_k. In the actual geometry the correction factor for A_2 was $Q_2 = 0.965$ and for A_4 was $Q_4 = 0.886$.

The transmission (of the backing in the backward geometry and of the fragment detector for the fraction c_{RF} in the forward geometry) was estimated from tabulated γ-ray attenuation coefficients.[12] It was estimated that about 10% of the heavy fragments were counted in the light fragment group and vice versa, and this overlap was taken into account in the theoretical expressions Eqs. (4a) and (4b).

V. RESULTS

The angular distribution in forward and backward geometries is shown for some typical cases in Fig. 2, where the label K corresponds to energy intervals as listed in Table I. The errors in the experimental points, and in the parameters found in the iterative least-squares fits, are standard deviations and include statistical errors only. The errors in the derived quantities are found from the error matrix. Systematical errors are included only when stated. The expressions (4a) and (4b) are only meaningful for a relatively high value of the correction factor g, and consequently they are used for energies above 0.290 MeV and their sum (4c) for lower energies. In both cases the coefficients A_{2F} and A_{4F} are free parameters, where we set $A_2 \equiv A_{2H} \equiv A_{2L}$ and $A_4 \equiv A_{4H} \equiv A_{4L}$. In the first case the number of γ rays per N_0 heavy

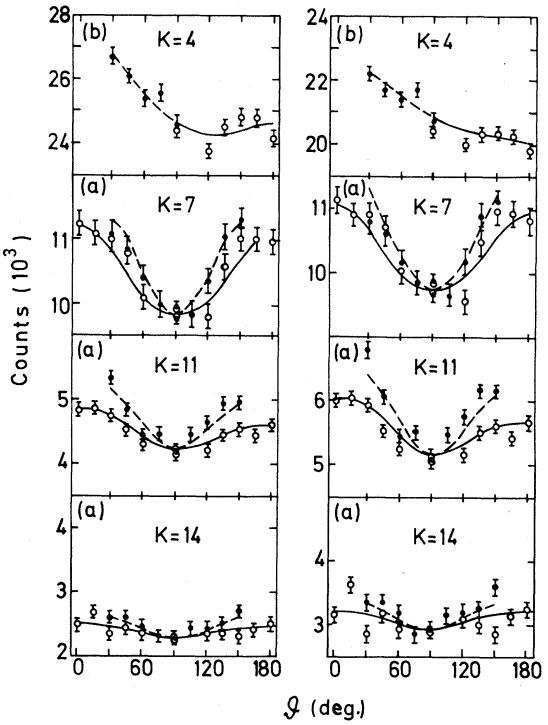

FIG. 2. (a) Angular distributions of the γ rays relative to the direction of motion of the light fragments in forward (dots) and backward (circles) geometrics with Ni ($K=11$) and Pt ($K=7$, 14) backing. The curves correspond to least-squares fits (forward geometry: dashed curves; backward geometry: solid curves). (Left: original data; right: data transformed by the inverse response matrix of the γ-ray detector.) (b) The same as under (a), but with the data for the two fragment groups added together (Ni backing).

and light fragment counts c_H and c_L, respectively, and in the second case the number of γ rays per $2N_0$ fragment counts c_F are found. The velocity attenuation factor F_B is either taken from Ref. 7 or is a free parameter. A normalization constant which takes into account the difference between the experimental and the nominal values of the γ-ray transmission in the two geometries, is set equal to unity in the first case, but is a free parameter in the second case. The curves in Fig. 2 correspond to the fits found.

The fraction of γ rays emitted from the heavy fragment group $[a_H = c_H/(c_H + c_L)]$ and the coefficients A_2 and A_4 versus γ-ray energy are shown in Figs. 3 (Pt backing) and 4 (Ni backing). The anisotropy $[A = W(0°)/W(90°) - 1]$ as a function of γ-ray energy is presented in Fig. 5 and Table I. The effect of the transformation from the pulse height to the energy distribution on these parameters is demonstrated in Fig. 3. It is indicated that the fraction a_H and the coefficient A_4 as a function of γ-ray energy have a structure which is reproducible. It is seen that the coefficient A_2 and the anisotropy A are small and even negative at low energies, reach a maximum at energies of about 0.50–0.65 MeV, and get gradually smaller at higher energies.

The number of γ rays per energy interval per fission N_γ can be found from the parameter c_F for $E_\gamma \leq 0.290$ MeV and from the sum $c_H + c_L$ for $E_\gamma \geq 0.290$ MeV through the corresponding efficiencies and the solid angle; see Table I. The error in the number and energy of the γ rays integrated

TABLE I. Number and anisotropy of γ rays emitted within 12 ns after fission, measured with Pt and Ni backings for various energy intervals.

K	Energy intervals (MeV)	N_γ (γ rays/fission) Pt	Ni	Anisotropy $[W(0°)/W(90°)-1]$ Pt	Ni
1	0.114 – 0.152	0.58	0.59	−0.089 ± 0.017	−0.095 ± 0.014
2	0.152 – 0.190	0.79	0.81	−0.040 ± 0.013	−0.037 ± 0.012
3	0.190 – 0.240	0.98	0.97	0.018 ± 0.012	0.016 ± 0.011
4	0.240 – 0.290	0.74	0.74	0.003 ± 0.013	0.024 ± 0.013
5	0.290 – 0.353	0.79	0.78	0.084 ± 0.009	0.059 ± 0.010
6	0.353 – 0.416	0.73	0.71	0.114 ± 0.009	0.136 ± 0.011
7	0.416 – 0.491	0.71	0.69	0.178 ± 0.009	0.197 ± 0.011
8	0.491 – 0.566	0.65	0.64	0.232 ± 0.010	0.273 ± 0.012
9	0.566 – 0.654	0.63	0.62	0.238 ± 0.010	0.243 ± 0.013
10	0.654 – 0.742	0.47	0.47	0.206 ± 0.011	0.171 ± 0.014
11	0.742 – 0.843	0.40	0.40	0.191 ± 0.012	0.199 ± 0.015
12	0.843 – 0.956	0.31	0.31	0.199 ± 0.014	0.192 ± 0.017
13	0.956 – 1.08	0.25	0.24	0.134 ± 0.015	0.120 ± 0.018
14	1.08 – 1.22	0.23	0.23	0.132 ± 0.016	0.068 ± 0.019
15	1.22 – 1.37	0.21	0.20	0.101 ± 0.016	0.118 ± 0.020
16	1.37 – 1.90	0.49	0.49	0.081 ± 0.011	0.120 ± 0.013
17	1.90 – 2.54	0.37	0.37	0.038 ± 0.012	0.032 ± 0.015
18	≥2.54	0.43	0.43	0.071 ± 0.012	0.039 ± 0.014
	≥0.114	9.76 ± 0.4	9.70 ± 0.4	0.091 ± 0.005	0.093 ± 0.005

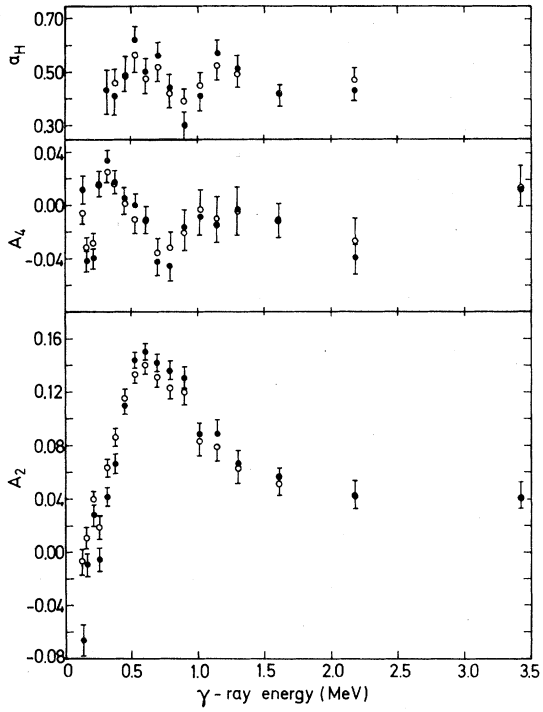

FIG. 3. The fraction of γ rays emitted from the heavy fragment group a_H and the coefficients A_2 and A_4 versus γ-ray energy as obtained with Pt backing from the original (circles) and the transformed (dots) data.

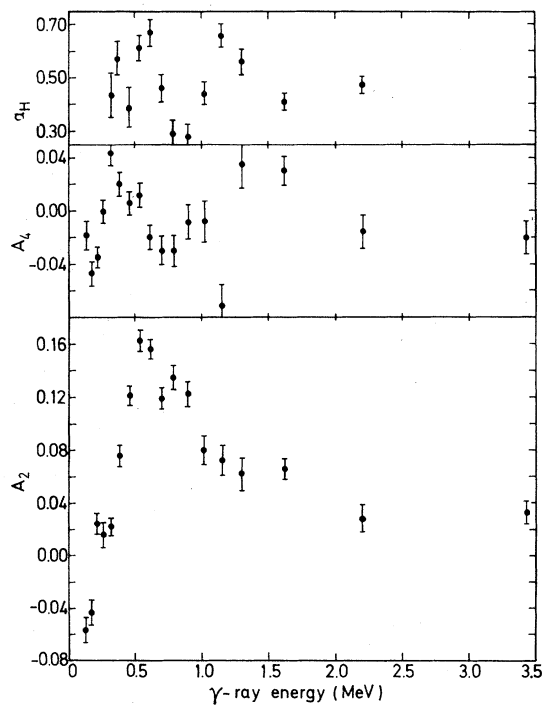

FIG. 4. The fraction of γ rays emitted from the heavy fragment group a_H and the coefficients A_2 and A_4 versus γ-ray energy as obtained with Ni backing from the transformed data.

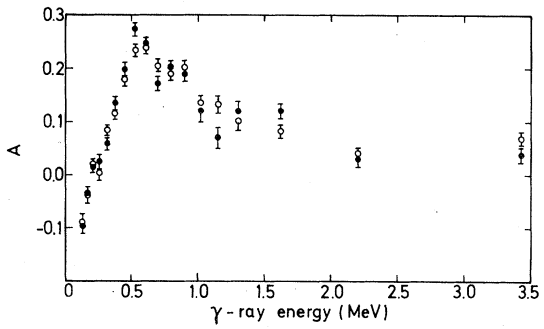

FIG. 5. The anisotropy versus γ-ray energy from the measurements with Pt (circles) and Ni (dots) backing. A tabulation of these data is presented in Table I.

over the whole spectrum is mainly due to the unfolding of the spectra and the calibration of the efficiency. Other systematical and statistical errors are much smaller. The combined error is estimated to be 0.4 in the total number and 0.3 MeV in the total energy. The integrated number of γ rays $N_{\gamma T}$ and the corresponding energy $E_{\gamma T}$ are given as a function of the lower γ-ray energy integral limit in Fig. 6 together with the results

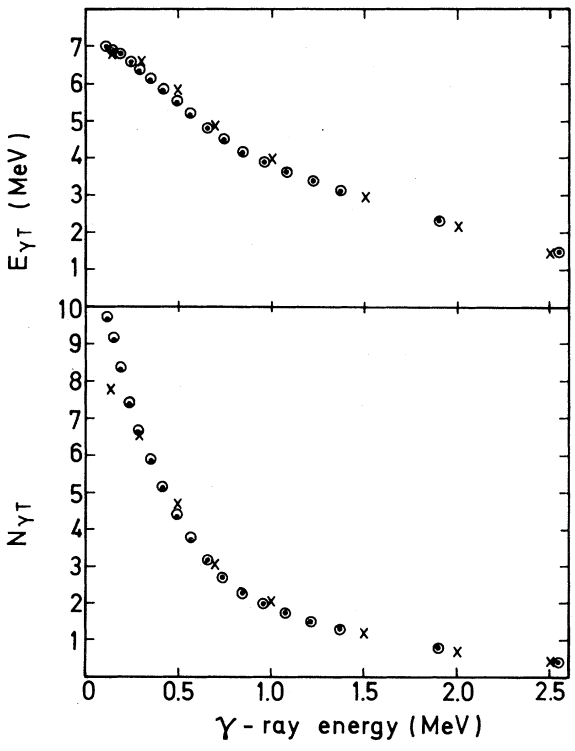

FIG. 6. The integrated number of γ rays per fission $N_{\gamma T}$ and the integrated γ-ray energy per fission $E_{\gamma T}$ versus γ-ray energy from the measurements with Pt (circles) and Ni (dots) backing compared with the corresponding results of Verbinski *et al.* (Ref. 13) (crosses).

TABLE II. Integrated numbers and energies and average asisotropies of γ rays for various energy ranges.

γ-ray energy range (MeV)	$N_{\gamma T}$ (γ rays/fission)	$E_{\gamma T}$ (MeV/fission)	Anisotropy $[W(0°)/W(90°)-1]$
	Present work		
	Thick Pt backing		
≥ 0.290	6.68	6.37	0.146 ± 0.005
0.114–0.290	3.09	0.62	-0.021 ± 0.011
≥ 0.114	9.76 ± 0.4	6.99 ± 0.3	0.091 ± 0.005
	Thick Ni backing		
≥ 0.290	6.59	6.33	0.147 ± 0.005
0.114–0.290	3.11	0.62	-0.018 ± 0.009
≥ 0.114	9.70 ± 0.4	6.95 ± 0.3	0.093 ± 0.005
	Others		
0.3–10.0 [a]	6.53	6.56	
0.14–0.3 [a]	1.270	0.282 ± 0.007	
0.14–10.0 [a]	7.80 ± 0.4	6.84 ± 0.3	
≥ 0.3 [b]			0.129 ± 0.005
≥ 0.100 [c]			0.11 ± 0.01
0.120–1.5 [d]			0.11 ± 0.01
0.120–1.5 [e]			0.052 ± 0.001

[a] Reference 13.
[b] Thick Pt backing (Refs. 5 and 6).
[c] Thin Al backing (Ref. 2).
[d] Thick Pt backing (Ref. 3).
[e] Thick Fe backing (Ref. 3).

of Verbinski *et al.*,[13] and the results are summarized in Table II. Here the average γ-ray energy for $E_\gamma \geq 2.54$ MeV is taken to be 3.43 MeV (cf. Ref. 13). The results of the two experiments are in good agreement for energies above about 0.3 MeV, but deviations are obtained at lower energies. Referred to the lower limit 0.14 MeV used in the experiment of Verbinski *et al.*,[13] the present experiment gives as an average for the two backings for the total number $N_{\gamma T} = 9.35$, and for the total energy $E_{\gamma T} = 6.92$ MeV. It follows that while the values of the total energy differ by only 0.08 MeV in the two experiments (with a combined error of 0.4 MeV), the values of the total number differ by 1.55 (with a combined error of 0.6).

The anisotropy for $E_\gamma \leq 0.290$ MeV is in fair agreement with the result of an integral measurement[5] (see Table II). The anisotropy as a function of γ-ray energy (see Figs. 3 and 4 and Table I) as well as the anisotropy averaged over the

TABLE III. Integral quantities associated with the heavy and the light fragments.

Energy range (MeV)	a_H	$N_{\gamma TH}$ (γ rays/fission)	$N_{\gamma TL}$ (γ rays/fission)	$E_{\gamma TH}$ (MeV/fission)	$E_{\gamma TL}$ (MeV/fission)
		Present work			
		Pt backing			
0.29–2.54	0.472 ± 0.014	2.95	3.30	2.27	2.63
		Ni backing			
0.29–2.54	0.485 ± 0.015	2.99	3.17	2.30	2.55
		Others			
≥ 0.3 [a]	0.40 ± 0.03				
0.09–10.0 [b]	0.44 [c]	2.88 ± 0.3	3.63 ± 0.4	2.66 ± 0.3	3.78 ± 0.4

[a] Reference 5.
[b] Fission of $^{235}U + n_{th}$ (Ref. 11).
[c] Obtained from the actual values of $N_{\gamma TH}$ and $N_{\gamma TL}$.

whole spectrum (see Table II) is in qualitative agreement with the results of Val'skii *et al.*[2] No significant difference in the anisotropy as measured with a nonmagnetic (Pt) and a magnetic (Ni) backing was found (see Figs. 3 and 4 and Tables I and II). The results of the present experiment therefore do not confirm the results of Lajtai *et al.*[3] who found a significant difference in the anisotropy when measured with a nonmagnetic (Pt) and a magnetic (Fe) backing (see Table II).

Integrated numbers $N_{\gamma TF}$ and energies $E_{\gamma TF}(F=H,L)$ associated with the two fragment groups and the fraction of γ rays emitted from the heavy fragment group are presented in Table III. The results obtained for the fraction of γ rays emitted from the heavy fragment group substantiate the earlier[5,11] results that more γ rays are emitted from the light than from the heavy fragment group.

VI. STATISTICAL-MODEL ANALYSIS

Parameters in the statistical model will here be fitted to the experimental results. Input parameters are for the heavy (light) fragment group the number of γ rays per energy interval $N_{\gamma H}(N_{\gamma L})$, where $N_{\gamma H}=a_H N_\gamma$ and $N_{\gamma L}=(1-a_H)N_\gamma$, and the coefficients A_2 and A_4, see Table I and Figs. 3 and 4. For γ-ray energies $E_\gamma \leq 0.290$ MeV and $E_\gamma \geq 2.54$ MeV it is assumed that $a_H \equiv 0.5$. Stretched E2 cascades[14,4] (i.e., the angular momentum is decreased by the maximum amount in each transition) are allowed from the even-even fragments, and stretched transitions at the low energy end of the γ-ray spectrum will be considered.

A. General

The initial angular momentum distribution of the fragment has been predicted to be of the form[15-17]

$$P(J) \propto (2J+1)\exp(-J(J+1)/B^2)\,, \tag{9}$$

where J represents the angular momentum, and B is related to inertial parameters and to the nuclear temperature. This distribution has a root mean square (rms) value of J approximately equal to $B-\frac{1}{2}$.

It has been shown[1,4] that the angular momentum initially is aligned, as predicted,[18] in a plane perpendicular to the direction of fission, i.e., $m=0$, where m is the projection of the angular momentum on the direction of fission which is taken as the quantization axis. Let $\vec{L}$ be the angular momentum of the photon and M its projection on the direction of $\vec{J}$. According to the statistical model[18] the probability of emission as a function of M for a given value of L ($L=1$, 2, or 3, i.e., dipole, quadrupole, or octupole radiation) is

$$w_M \propto \exp(-(\vec{J}-\vec{L})^2/2\sigma^2) \propto \exp(JM/\sigma^2)\,. \tag{10}$$

Theoretically the spin cutoff parameter σ is

$$\sigma^2 = \mathcal{I}T/\hbar^2\,, \tag{11}$$

where $\mathcal{I}$ is the moment of inertia and T is the nuclear temperature. In the present analysis σ will not be directly evaluated using Eq. (11) but treated as a parameter.

The general form of the angular distribution in the c.m. system [cf. Eq. (8)] is a sum of even Legendre polynomials[19]

$$W(\theta) = \sum A_k P_k(\cos\theta)\,, \tag{8a}$$

where

$$A_k = B_k U_k F_k\,. \tag{12}$$

Here F_k depends on the angular momentum properties of the transition, B_k is the orientation parameter for the initial state, and U_k is a parameter which indicates the change in orientation due to preceding decays. If there are several γ rays in cascade U_k is given by

$$U_k = U_k^1 U_k^2 \ldots\,. \tag{13}$$

It should be noted that the angular distributions of the γ rays in a stretched cascade of the form $J \to J-L \to J-2L \to \ldots$ are the same for all the transitions.[20] The angular distribution in the statistical model is obtained by weighting the coefficients A_k in Eq. (8a) by the weighting factors given by Eq. (10). The angular distribution in the classical limit in the statistical model is given elsewhere.[18,5,6]

B. Special assumptions

It will here be assumed that the prompt neutrons are emitted before any of the faster γ-ray transitions have occurred (cf. Refs. 7 and 21). The distribution of the numbers of neutrons per fission are replaced by average values[22-24] ($\nu_H=1.60$, $\nu_L=2.13$). The intrinsic spin of the neutrons is neglected. For simplicity it will be assumed that the probability distribution as given by Eq. (10) also can be applied to neutron emission using for the parameter σ a value of 4 (cf. Ref. 1), and where $L=1$ and $L=2$ with equal probability for the first neutron, and $L=1$ for the succeeding neutron(s).

The time of emission of the γ rays is assumed to increase with decreasing γ-ray energy as the general trend is (cf. Ref. 7). The distribution of the numbers of γ rays about their mean is tentatively taken into account. Dipole and quadrupole transitions are considered, but not octupole and mixed transitions. The parameter σ for γ ray emission (hereafter called σ_γ) is taken to be a

constant during the deexcitation. For even values of J the first γ ray is assumed to populate levels which give rise to all the stretched E2 cascades[4] characteristic of even-even fragments, in a fraction f_{str} of the cases, and levels which decay by statistical transitions, in a fraction $1-f_{str}$ of the cases where we here set $f_{str}=0.5$. This means that the number of stretched E2 cascades N_{str} and the angular distribution of the γ rays in the cascades are determined when the first γ ray is emitted. Transitions from levels with $J=0$ are assumed not to take place. It follows that a cascade is terminated when a zero angular momentum ($J=0$) is attained. After the emission of all the γ rays in the actual time range (here within 12 ns after fission) a given fraction of the cascades f_0 has ended at a level with $J=0$, where we here set $f_0=0.95$, and where the remaining fraction of $1-f_0$ is assumed to be accounted for by the emission of electrons,[14] and by the emission of γ rays at longer times[8] or (and), with energy lower than 0.114 MeV.

C. Calculation

The initial angular momentum distribution is defined by the parameter B, see Eq. (9), and the initial alignment is taken to be complete. With the assumptions made, the values of the parameters U_k^1 (U_k^2) after the emission of the first (second) neutron, where $k=2,4$, can be calculated by means of the weight factors w_M given by Eq. (10), and the resulting values of U_k can be found, see Eq. (13). The angular momentum distribution after the emission of the first (second) neutron can be calculated from the preceding distribution by means of the weight factors w_M. For the average value of the number of neutrons ν_F the values of the parameters U_k as well as the angular momentum distribution are found by linear interpolation.

The final angular momentum distribution and the alignment of the fragments after all the neutrons have been emitted, define the initial distribution and the alignment at the start of the γ-ray deexcitation. The parameters in the model which can be determined for energy interval number K (see Table I) are for any values of the parameters B and σ_γ, the fraction of the statistical dipole and the statistical quadrupole and the stretched E2 transitions in cascade, c_{1K}, c_{2K}, and c_{3K}, respectively, where $c_{1K}+c_{2K}+c_{3K}=1$, and $c_{iK}\leq 0$ for $i=1$, 2, and 3. While the first γ rays deexcite levels well above the yrast line,[25] the last γ rays deexcite levels at or near to the yrast line and are each forced to reduce the angular momentum of the nucleus. The two former fractions are therefore assumed to represent not statistical, but rather stretched transitions for γ-ray energies lower than E'_γ, where we here set $E'_\gamma=0.240$ MeV. The calculation for the nth ray is done in three steps. The first step is the calculation of the coefficients A_k averaged over the angular momentum distribution. As noted above, the coefficients A_k in stretched cascades are unchanged throughout the cascade and are calculated only for the first γ ray in the cascade. The second step is to find the fractions c_{1K}, c_{2K}, and c_{3K} by a linear least-squares fit for all values of the index K which correspond to the nth γ ray. The third step is to find the resulting values of the parameters U_k and the angular momentum distribution, and is done only for the two former components using average values of the fractions of dipole and quadrupole transitions. Here the parameters U_k are found from Eq. (13) where the parameters U_k^n are calculated with the actual weight factors w_M [cf. Eq. (10) for statistical transitions], weighted by the fractions of dipole and quadrupole transitions and finally averaged over the angular momentum distribution. The angular momentum distribution is calculated from the preceding distribution by means of the actual weight factors w_M and is finally weighted by the fractions of dipole and quadrupole transitions. The procedure can then be repeated for the next and all the succeeding γ rays. A first run is made with the energy intervals (see Table I) grouped together to represent average numbers of γ rays ($K=18$–13, 12–9, 8–6, 5–4, and 3–1). Figure 7 presents an example of the calculated values of the parameters $U_k(k=2,4)$. A second run is subsequently made with the energy intervals grouped together to represent the distribution of the numbers of γ rays ($K=18$–13, 12–9, 8–7, 6–5, 4, 3, 2, and 1), and where the values

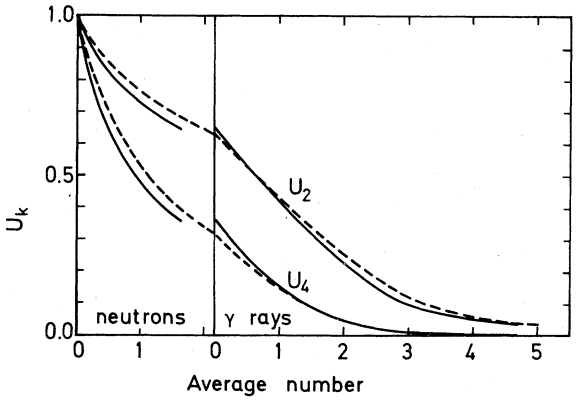

FIG. 7. The parameters U_2 and U_4 as calculated (and interpolated between integer values of the numbers) for the statistical part at various stages of the deexcitation of heavy fragments (solid curves) and light fragments (dashed curves).

of U_k are interpolated between the values found in the first run.

By an iterative procedure where runs with different pairs of values of the parameters B and σ_γ are made, a consistent set of parameters (B, σ_γ, c_{1K}, c_{2K}, and c_{3K} where $K=18-1$) is finally determined by the two requirements:

(a) The fraction of the cascades f which ends at a level with angular momentum $J=0$ is equal to the predetermined value $f_0=0.95$.

(b) The total number of stretched E2 cascades found is equal to the number N_{str} as determined after the emission of the first γ ray.

Figure 8 presents angular distribution coefficients of γ rays in stretched and statistical transitions and in stretched cascades at various stages of the deexcitation. Figure 9 presents an example of the fractions c_{iK} of the actual components ($i=1-3$) in the various energy intervals ($K=18-1$) together with the fit obtained to the experimental values of the coefficients A_2 and A_4.

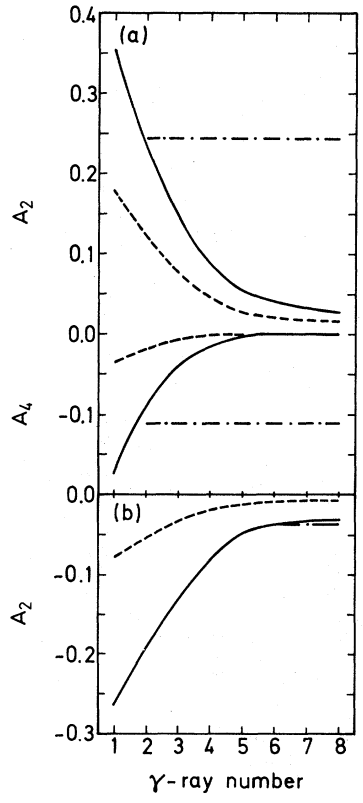

FIG. 8. (a) Angular distribution coefficients of quadrupole radiation at various stages of the deexcitation. The solid curves represent stretched transitions, the dashed curves statistical transitions, and the dot-dashed curves stretched cascases. (b) The same as under (a) but for dipole radiation.

D. Results and discussion

Figures 10 and 11 present in a schematic way, the partial and the total γ-ray energy spectra from the heavy and the light fragments, respectively, and the results are summarized in Table IV. It is seen that the dipole and the quadrupole components are about equally strong at high γ-ray energies, the dipole component predominates at low energies and the quadrupole component at intermediate energies. The quadrupole radiation can be assumed to be $E2$, an assumption which is consistent with the results of lifetime measurements.[7] The distribution of electric and magnetic dipole transitions as a function of γ-ray energy in known nuclei (cf. Ref. 2) indicates that the dipole radiation is mainly $M1$ at low energies and $E1$ at high energies. Components of stretched $E2$ cascades are seen in the energy ranges 0.15–0.24 MeV and 0.35–0.96 MeV. A weak anisotropy can thus possibly result if components with anisotropies of opposite signs are summed (for $E_\gamma \geq 1.90$ MeV and for $E_\gamma=0.15-0.29$ MeV), and at the low energy end of the spectrum (except in stretched cascades) also from dealignment caused

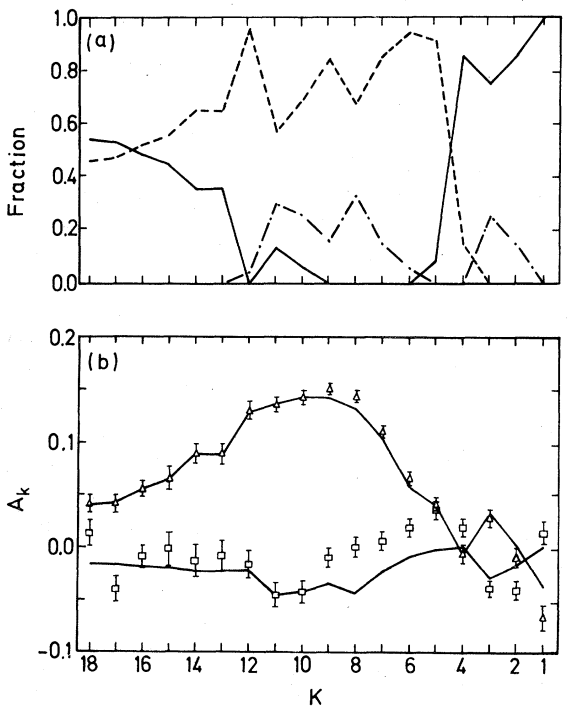

FIG. 9. (a) The derived fractions of γ rays emitted in dipole (solid curves) and quadrupole (dashed curves) transitions and in stretched $E2$ cascades (dot-dashed curves) versus the index K. (b) The corresponding calculated values of A_2 and A_4 (curves) together with the experimental values of A_2 (triangles) and A_4 (squares). Here $B=6.50$ and $\sigma_\gamma=2.43$.

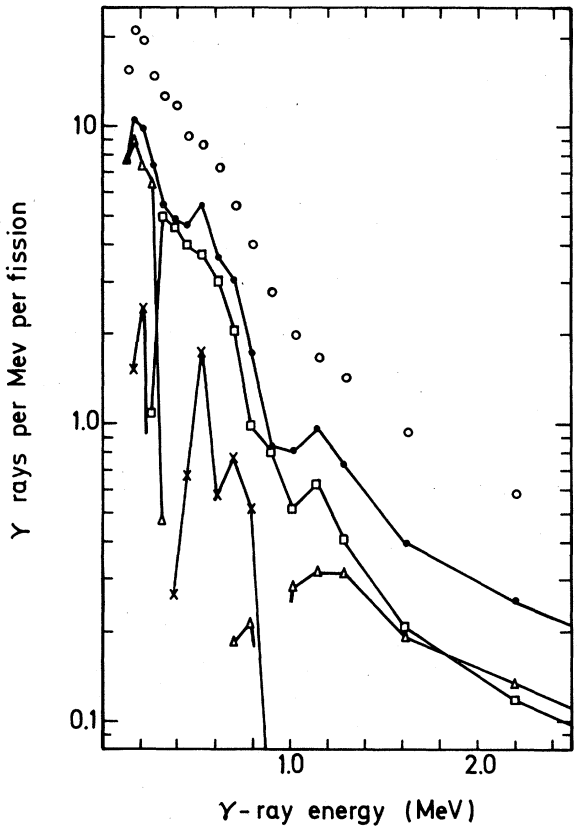

FIG. 10. The spectrum of γ rays from the heavy fragments (dots) and the spectra associated with dipole (triangles) and quadrupole (squares) transitions and stretched $E2$ cascades from even-even fragments (crosses). For γ-ray energies $E_\gamma \leq 0.290$ MeV and $E_\gamma \geq 2.54$ MeV it is assumed that $a_H \equiv 0.5$. The total γ-ray energy spectrum (circles) is given for reference. (Pt backing.) The curves are drawn only to guide the eye.

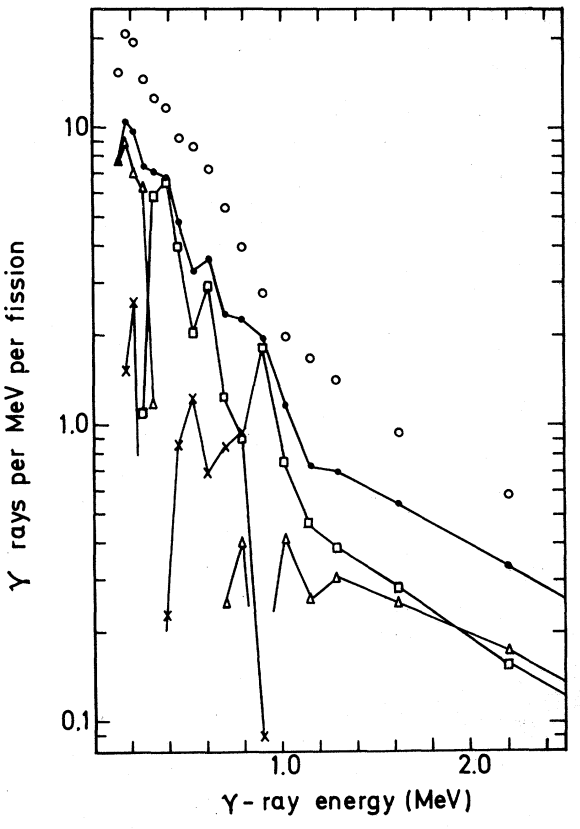

FIG. 11. The same as for Fig. 10, but for the light fragments.

by preceding decays (cf. Fig. 7). The relative yields of the $2^+ \rightarrow 0^+$, $4^+ \rightarrow 2^+$, $6^+ \rightarrow 4^+$, and $8^+ \rightarrow 6^+$ transitions in the $E2$ cascades (averaged over both fragment groups) as obtained with the present model are in the ratio 100 : 71 : 40 : 18 (averaged over both data sets) compared with 100 : 68 : 35 : 15 for the relative yields of transitions in the ground-state bands of even-even fragments.[4] The model further gives, for the angular distribution coefficients when averaged over the $2^+ \rightarrow 0^+$ and $4^+ \rightarrow 2^+$ transitions, $A_2 = 0.27$ and $A_4 = -0.15$ (averaged over both data sets), while the corresponding average values for specific γ rays from even-even fragments[4] are $A_2 = 0.27$ and $A_4 = -0.07$. A striking feature in the results is the strong anisotropies in the energy range 0.42–0.96 MeV (see Table I and Fig. 5). In this energy range the half-lives averaged over all fragments are lying in the time region $2 \times 10^{-13} - 3 \times 10^{-11}$ s.[7] The γ rays associated with the ground-state rotational bands have typically energies below 0.60 MeV.[4] The $2^+ \rightarrow 0^+$ half-lives are in the time region 10^{-10}–10^{-9} s,[14] but the half-lives of the higher band members are substantially shorter. On the other hand the γ-ray

TABLE IV. Derived values of the angular momentum parameter B and the spin cutoff parameter σ_γ with the corresponding average values of the angular momentum and the fractions of γ rays emitted in dipole and quadrupole transitions and in stretched $E2$ cascades from even-even fragments.

	Heavy fragments		Light fragments	
	Pt	Ni	Pt	Ni
B	6.50	6.59	7.25	7.14
σ_γ	2.43	2.50	2.33	2.41
J_{rms} $(\hbar)$ [a]	6.09	6.17	6.83	6.72
$\bar{J}$ $(\hbar)$ [a]	5.29	5.37	5.95	5.85
J^*_{rms} $(\hbar)$ [b]	5.63	5.71	6.19	6.09
$\bar{J}^*$ $(\hbar)$ [b]	4.81	4.88	5.29	5.21
$\langle c_1 \rangle$	0.384	0.368	0.383	0.369
$\langle c_2 \rangle$	0.499	0.514	0.498	0.510
$\langle c_3 \rangle$	0.117	0.118	0.119	0.120

[a] Primary angular momentum.
[b] Postneutron angular momentum.

energy spectrum associated with vibrational transitions (cf. Ref. 26) in even-even nuclei extends well above 0.6 MeV, and the half-lives are of the order of 10^{-11} s. While the components of the stretched $E2$ cascades (see Figs. 10 and 11) at the lower energies can be accounted for by the transitions in the ground-state rotational bands of even-even fragments,[4] it is indicated that a large part of the components in the energy range 0.57–0.96 MeV can be associated with vibrational transitions in even-even fragments.

One of the results is that the light fragments have greater angular momentum than the heavy fragments. A limitation in this type of experiment is that the coefficients A_{kH} and $A_{kL}(k=2,4)$ cannot be determined independently and therefore are assumed to be equal. It is noted that measurements made with the collimator technique which do not have this type of limitation, but cover only about 30% of the γ rays, show little difference in the anisotropy for the two fragment groups.[27] The average angular momentum $\bar{J}$ in this model decreases linearly with the number of γ rays emitted, and with about $1.0\hbar$ per γ ray. The greater angular momentum of the light fragments then follows mainly from the higher number of γ rays in that group. The present result cannot, however, be directly compared with the result of Wilhelmy *et al.*[1] for even-even fission fragments that the heavy fission fragments have about 20% greater angular momentum than the light fragments. Averaged over both fragment groups the results are rather independent of the above limitation.

The error in the total number of γ rays per fission of ± 0.4 contributes with an error of ± 0.3 in the parameter B and an error of ∓ 0.1 in the parameter σ_γ. Deviations from the assumed sequence of emission of neutrons and (or) γ rays affect the results averaged over the whole γ-ray spectrum only insignificantly. An error in the number of neutrons per fragment $\nu_F(F=H,L)$ and (or) in the fraction of γ rays from the heavy fragments a_H is of opposite sign for the two fragment groups, and cancels out when averaged over all fragments. The distribution of the numbers of γ rays is assigned an error equivalent to ± 1 γ ray in the maximum number, which gives an error of ± 0.1 in B and an error of $^{0.4}_{0.1}$ in σ_γ. The omission of octupole and mixed transitions in the analysis is assumed to contribute with an error of ± 0.3 in B and an error of ± 0.2 in σ_γ. The fraction f_{str} is assigned an error of ± 0.1 which gives an error of ∓ 0.13 in B, an error of ± 0.16 in σ_γ and an error of ± 0.24 in the number of γ rays in E2 cascades. The assumption that transitions from levels with $J=0$ do not take place is justified at or near to the yrast line, but not well above it. It should also be noted that if both initial and final state have $J=0$, no single photon emission can occur. The error due to the above assumption is assumed to be ± 0.3 in B and ± 0.2 in σ_γ. The fraction f_0 is assigned an error of $^{+0.02}_{-0.05}$ which gives an error of $^{-0.08}_{+0.20}$ in B and an error of $^{-0.06}_{+0.15}$ in σ_γ. The energy at which the spectrum loses its character as an evaporation spectrum E'_γ is assigned an error of ± 0.10 MeV, which gives an error of ± 0.08 in B and an error of ∓ 0.06 in σ_γ. The approximations inherent in the weight factors w_M as given by Eq. (10) are assumed to contribute with an error of ± 0.5 in B and an error of $^{+0.5}_{-0.3}$ in σ_γ. The combined error in the parameter σ_γ is then $^{+0.8}_{-0.5}$ and the combined error in the parameter B is ± 0.8 which gives an error of $\pm 0.8\hbar$ and $\pm 0.7\hbar$ in the rms value and the average value of the postneutron angular momentum, respectively. An assigned error of $^{+0.8}_{-0.5}$ in the parameter σ for neutron emission gives an error of ∓ 0.25 in the parameter B. The use of Eq. (10) for neutron emission is assumed to contribute with an error of ± 0.5 in B. An error of ∓ 0.2 in B is due to an assigned error of ± 0.5 in the fraction of the cases in which the first neutron is emitted with an angular momentum $L=1$ (and with $L=2$ in the remaining fraction of cases), or to an equivalent error for the second or all neutron(s). The combined error in B associated with neutron emission is then ± 0.6, and the total combined error in B is ± 1.0, which gives an error of $\pm 1.0\hbar$ and $\pm 0.9\hbar$ in the rms value and the average value of the primary angular momentum, respectively. Errors due to deviations from the functional form of the initial angular momentum distribution as given by Eq. (9) and from complete initial alignment ($m=0$) have here not been taken into account. If the pre-exponential term in the angular momentum distribution as given by Eq. (9) is changed from $2J+1$ to $(2J+1)^2$, the rms value of the primary angular momentum is changed by $-0.45\hbar$ and the value of the parameter σ_γ by 0.10. Partial initial alignment can be taken into account by multiplying the angular distribution coefficients $A_k(k=2,4)$ by attenuation coefficients $\alpha_k(J)$,[28] which are rather independent of the angular momentum. Under the assumption of a Gaussian distribution of the substates centered around $m=0$ and with a standard deviation in the distribution of 0.2 in units of the angular momentum we have with good approximation $\alpha_2(J)=0.9$ and $\alpha_4(J)=0.7$ (see Ref. 28), which compared with complete alignment ($m=0$) gives a change of $0.5\hbar$ in the primary angular momentum and a change of -0.15 in the parameter σ_γ.

We then get (averaged over both data sets) for the rms value of the primary and the postneutron angular momentum $J_{\text{rms}}=(6.5\pm 1.0)\hbar$ and J^*_{rms}

TABLE V. Average angular momentum $\bar{J}$ (in units of $\hbar$).

	Present experiment	Theory [a]		
		Adiabatic	$kT=1$ MeV	$kT=2$ MeV
Heavy fragments	5.3	4.2	4.5	5.1
Light fragments	5.9	5.0	5.3	6.1
All fragments	5.6	4.6	4.9	5.6

[a] The theoretical results are for the even-even fragments of fission of ^{236}U (Ref. 29).

$=(5.9\pm0.8)\hbar$, respectively. The corresponding average values are $\bar{J}=(5.6\pm0.9)\hbar$ and $\bar{J}^*=(5.0\pm0.7)\hbar$, respectively. Implicitly a level with zero angular momentum reached in the γ-ray deexcitation of the fragments has been identified with the ground state. The average values of the angular momentum given must therefore be referred to the average angular momentum of the fragments in the ground state. Wilhelmy *et al.*[1] concluded from a statistical-model analysis that the primary angular momentum of even-even fragments was $J_{\rm rms}=(7\pm2)\hbar$, using for the spin cutoff parameter a value of $\sigma_\gamma=3$. For the spin cutoff parameter we get $\sigma_\gamma=2.4^{+0.8}_{-0.5}$. The nuclear temperature is poorly known at low excitation energies, but it is indicated that the moment of inertia, see Eq. (11), is rather smaller than the rigid body moment of inertia (cf. Refs. 5 and 2). We further get that the statistical transitions (stretched for 0.114 MeV $\leqq E_\gamma \leqq$ 0.240 MeV) account for 8.6 γ rays per fission [3.7 γ rays (38%) as dipole and 4.9 γ rays (50%) as quadrupole radiation], and that 1.2 γ rays per fission (12%) are emitted in stretched E2 cascades from even-even fragments.

E. Comparison with theory

In Table V the present results for the average angular momentum $\bar{J}$ of the heavy and the light fragments are compared with a theoretical model,[29] in which it is assumed that only the bending modes carry angular momentum at scission, and with the numerical calculations being done for the even-even fragments of fission of ^{236}U. Post scission angular momentum introduced from Coulomb repulsion effects has here been neglected, but has been calculated to be 10 to 20% of the angular momentum at the scission point.[29] Insofar as the results can be compared, satisfactory agreement is obtained for the adiabatic case and for the nonadiabatic case with a nuclear temperature at scission of $kT=1$ MeV.

[1] J. B. Wilhelmy, E. Cheifetz, R. C. Jared, S. G. Thompson, H. R. Bowman, and J. O. Rasmussen, Phys. Rev. C 5, 2041 (1972).

[2] G. V. Val'skii, B. M. Aleksandrov, I. A. Baranov, A. S. Krivokhatskii, G. A. Petrov, and Yu. S. Pleva, Yad. Fiz. 10, 240 (1969) [Sov. J. Nucl. Phys. 10, 137 (1969)].

[3] A. Lajtai, L. Jéki, Gy. Kluge, I. Vinnay, F. Engard, P. P. Dyachenko, and B. D. Kuzminov, in *Proceedings of the Symposium on Physics and Chemistry of Fission, Rochester, 1973* (IAEA, Vienna, 1974), Vol. II, p. 249.

[4] A. Wolf and E. Cheifetz, Phys. Rev. C 13, 1952 (1976).

[5] K. Skarsvåg and I. Singstad, Nucl. Phys. 62, 103 (1965).

[6] K. Skarsvåg, Nucl. Phys. A96, 385 (1967).

[7] K. Skarsvåg, Nucl. Phys. A253, 274 (1975).

[8] K. Skarsvåg, Nucl. Phys. A153, 82 (1970).

[9] J. S. Fraser, J. C. D. Milton, H. R. Bowman, and S. G. Thompson, Can. J. Phys. 41, 2080 (1963).

[10] S. H. Vegors, Jr., L. L. Marsden, and R. L. Heath, AEC Reseacch and Development Report No. IDO-16370, 1958, p. 51.

[11] F. Pleasonton, R. L. Ferguson, and H. W. Schmitt, Phys. Rev. C 6, 1023 (1972).

[12] C. M. Davisson, in *Alpha-, Beta-, and Gamma-Ray Spectroscopy*, edited by K. Siegbahn (North-Holland, Amsterdam, 1965), Vol. 1, p. 827.

[13] V. V. Verbinski, H. Weber, and R. E. Sund, Phys. Rev. C 7, 1173 (1973).

[14] E. Cheifetz and J. B. Wilhelmy, *Nuclear Spectroscopy and Reactions*, edited by J. Cerny (Academic, New York and London, 1974), part C, p. 229.

[15] T. Ericson and V. Strutinskii, Nucl. Phys. 8, 284 (1958); 9, 689 (1958).

[16] J. R. Nix and W. J. Swiatecki, Nucl. Phys. 71, 1 (1965).

[17] J. O. Rasmussen, W. Nörenberg, and H. J. Mang, Nucl. Phys. A136, 456 (1969).

[18] V. M. Strutinskii, Zh. Eksp. Teor. Fiz. (USSR) 37, 861 (1959) [Sov. Phys. JETP 10, 613 (1960)].

[19] R. J. Blin-Stoyle and M. A. Grace, *Handbuch der Physik*, edited by S. Flügge (Springer, Berlin, 1957), Bd. 42, p. 555.

[20] J. A. M. Cox and H. A. Tolhoek, Physica 19, 673 (1953).

[21] K. Skarsvåg, Phys. Rev. C 16, 1902 (1977).

[22] J. W. Boldeman, in *Proceedings of the International Specialists' Symposium on Neutron Standards and Applications, Gaithersburg, Maryland, 1977* [Nat.

Bur. Stand. (U.S.) Spec. Publ. 493, Washington, D. C., 1977], p. 182.
[23]H. R. Bowman, S. G. Thompson, J. C. D. Milton, and W. J. Swiatecki, Phys. Rev. 126, 2120 (1962).
[24]K. Skarsvåg, Phys. Scr. 7, 160 (1973).
[25]J. R. Grover and J. Gilat, Phys. Rev. 157, 814 (1967).
[26]S. A. E. Johansson, Nucl. Phys. 60, 378 (1964).
[27]P. Armbruster, H. Labus, and K. Reichelt, Z. Naturforsch. 26a, 512 (1971).
[28]T. Yamazaki, Nucl. Data Tables A3, 1 (1967).
[29]M. Zielinska-Pfabé and K. Dietrich, Phys. Lett. 49B, 123 (1974).